Magnetization reorientation induced by spin-orbit torque in YIG/Pt bilayers

Ying-Yi Tian(田颖异), Shuan-Hu Wang(王拴虎), Gang Li(李刚), Hao Li(李豪), Shu-Qin Li(李书琴), Yang Zhao(赵阳), Xiao-Min Cui(崔晓敏), Jian-Yuan Wang(王建元), Lv-Kuan Zou(邹吕宽), Ke-Xin Jin(金克新)

Citation: Chin. Phys. B . 2020, 29(11): 117504 . **doi:** 10.1088/1674-1056/abb666
Journal homepage: http://cpb.iphy.ac.cn; http://iopscience.iop.org/cpb

What follows is a list of articles you may be interested in

Phase diagrams and magnetic properties of the mixed spin-1 and spin-3/2 Ising ferromagnetic thin film:Monte Carlo treatment

B Boughazi, M Boughrara, M Kerouad

Chin. Phys. B . 2019, 28(2): 027501 . **doi:** 10.1088/1674-1056/28/2/027501

Effects of spacer layers on magnetic properties and exchange couplings of Nd-Fe-B/Nd-Ce-Fe-B multilayer films

Ya-Chao Sun(孙亚超), Ming-Gang Zhu(朱明刚), Wei Liu(刘伟), Rui Han(韩瑞), Wen-Chen Zhang(张文臣), Yan-Feng Li(李岩峰), Wei Li(李卫)

Chin. Phys. B . 2017, 26(10): 107501 . **doi:** 10.1088/1674-1056/26/10/107501

Low temperature ferromagnetic properties of CdS and CdTe thin films

Hafiz Tariq Masood, Zahir Muhammad, Muhammad Habib, Dong-Ming Wang(王东明), De-Liang Wang(王德亮)

Chin. Phys. B . 2017, 26(6): 067503 . **doi:** 10.1088/1674-1056/26/6/067503

Structure dependence of magnetic properties in yttrium iron garnet by metal-organic decomposition method

Yuan Liu(刘园), Xiang Wang(王翔), Jie Zhu(朱杰), Runsheng Huang(黄润生), Dongming Tang(唐东明)

Chin. Phys. B . 2017, 26(5): 057501 . **doi:** 10.1088/1674-1056/26/5/057501

Fabrication and magnetocrystalline anisotropy of NiCo(002) films

Fan Wei-Jia, Ma Li, Shi Zhong, Zhou Shi-Ming

Chin. Phys. B . 2015, 24(3): 037507 . **doi:** 10.1088/1674-1056/24/3/037507

Magnetization reorientation induced by spin–orbit torque in YIG/Pt bilayers*

Ying-Yi Tian(田颖异)[1], Shuan-Hu Wang(王拴虎)[1,†], Gang Li(李刚)[3], Hao Li(李豪)[1], Shu-Qin Li(李书琴)[1], Yang Zhao(赵阳)[1], Xiao-Min Cui(崔晓敏)[1], Jian-Yuan Wang(王建元)[1], Lv-Kuan Zou(邹吕宽)[2], and Ke-Xin Jin(金克新)[1,‡]

[1] *Shaanxi Key Laboratory of Condensed Matter Structures and Properties and MOE Key Laboratory of Materials Physics and Chemistry under Extraordinary Conditions, School of Science, Northwestern Polytechnical University, Xi'an* 710072, *China*

[2] *High Magnetic Field Laboratory, Chinese Academy of Sciences, Hefei* 230031, *China*

[3] *School of Science and Technology, Tianjin University of Finance and Economics, Tianjin* 300222, *China*

(Received 12 August 2020; revised manuscript received 31 August 2020; accepted manuscript online 9 September 2020)

In this work, we report the reorientation of magnetization by spin–orbit torque (SOT) in YIG/Pt bilayers. The SOT is investigated by measuring the spin Hall magnetoresistance (SMR), which is highly sensitive to the direction of magnetic moment of YIG. An external in-plane rotating magnetic field which is applied to the YIG/Pt bilayers, and the evolutions of SMR under different injected currents in the Pt layer, result in deviation of SMR curve from the standard shape. We conclude that the SOT caused by spin accumulation near the interface between YIG and Pt can effectively reorient the in-plane magnetic moment of YIG. This discovery provides an effective way to modulate YIG magnetic moments by electrical methods.

Keywords: spin–orbit torque, yttrium iron garnet, reorientation of magnetization, spin Hall magnetoresistance

PACS: 75.70.–i, 75.50.Gg, 75.70.Tj **DOI:** 10.1088/1674-1056/abb666

1. Introduction

Spin–orbit torque (SOT) has been experimentally and theoretically shown to be a useful method to modulate the magnetization orientation in nanoscale magnetic devices with currents, which are orders of magnitude lower than those required for magnetic field-based control.[1–7] The magnetization can be effectively manipulated by the current-induced SOT, and a torque is generated in the presence of large spin–orbit coupling (SOC). Due to the lower current density needed to reorient magnetic moment of ferromagnets, the conversion of magnetization with SOT effect can be observed intuitively via current flow.[8] The SOT is categorized into two generic torques, namely the field-like torque ($\tau_{\rm FL} = \boldsymbol{M} \times \boldsymbol{P}$, where $\boldsymbol{P}$ represents the non-equilibrium spin polarization direction and $\boldsymbol{M}$ represents the magnetic moment vector) and the antidamping torque ($\tau_{\rm DL} = \boldsymbol{M} \times (\boldsymbol{P} \times \boldsymbol{M})$).[9] The main effect of field-like torque is the same as that of the torque exerted by a uniform magnetic field, which causes the domain walls to reorient in the direction perpendicular to $\boldsymbol{P}$.[10] In contrast, the antidamping torque induces the magnetic domain walls to reorient in the in-plane direction.

The advent of SOT allows the electrical switching of a single ferromagnetic (FM) layer with perpendicular magnetic anisotropy (PMA) by a peripheral current.[5,9,11–16] The anomalous Hall effect is usually used in experiment to test the electrical switching.[17] Liu *et al.*[5] reported a giant spin Hall effect (SHE) in β-Ta that generates spin currents intense enough to induce efficient spin–torque switching of an out-of-plane polarized ferromagnet and an in-plane polarized ferromagnet at room temperature. Recently, Chen *et al.*[10,18] have reported the use of pulsed current to modulate the transition of Neel order in a NiO(001)/Pt heterostructure, and the detection of the transition by a new method based on spin Hall magnetoresistance (SMR). They found that the Neel order is reoriented towards the direction of writing current because of the antidamping torque. This discovery opens up an effective way to the studying of the SOT-induced reorienting phenomenon in other materials.

As a well-known room-temperature ferrimagnetic insulator with low damping coefficient and long magnon diffusion length,[19,20] the yttrium iron garnet ($Y_3Fe_5O_{12}$, YIG) has been widely studied in spintronics.[21] Heavy metal (HM)/YIG heterostructures exhibit many interesting phenomena such as spin Seebeck effect[22] and spin Hall magnetoresistance.[23,24] There are some rearches related to current-induced magnetization switching in YIG systems,[25,26] but in-plane magnetic moment conversion induced by SOT has been rarely studied. We postulate that the spin accumulation near the interface be-

*Project supported by the Natural Science Foundation of Shaanxi Province, China (Grant No. 2020JM-088), the National Natural Science Foundation of China (Grant Nos. 51572222, 51701158, and 51872241), and the Fundamental Research Funds for the Central Universities, China (Grant Nos. 3102017jc01001 and 310201911cx044).

†Corresponding author. E-mail: shwang2015@nwpu.edu.cn

‡Corresponding author. E-mail: jinkx@nwpu.edu

tween Pt and YIG will generate a torque acting on the YIG magnetic moment. Due to the fact that the SMR is strongly dependent on magnetization direction,[23,24,27] we investigate the SMR curves under different injected currents in Pt in this work. We find that the antidamping torques will reorient the YIG magnetic moment even when the external magnetic field is large enough to saturate the YIG magnetization.

2. Materials and methods

The YIG films with thickness of 5 nm and 3 nm were grown on 5 mm×5 mm GGG (111) substrates by pulsed laser deposition, and then 5-nm-thick Hall bar-shaped Pt was attached to the top of YIG by magnetron sputtering. The external magnetic field was applied to two directions, the first direction being parallel to, and the second direction being perpendicular to the transversal direction of the Hall bar. The coercivity values in both directions for the YIG(5 nm)/Pt and YIG(3 nm)/Pt samples are characterized by the longitudinal spin Seebeck effect induced inverse spin Hall effect voltage ($V_{\rm ISHE}$).[28–30] As shown in Figs. 1(a) and 1(b), both samples have small coercivities. Their magnetic moments can be saturated by small magnetic fields. The magnetization is almost uniform in different directions of the YIG(5 nm)/Pt sample, and the $V_{\rm ISHE}$–H curves in different directions nearly overlap each other. However, for the YIG(3 nm)/Pt sample, a rectangle-shaped M–H loop is obtained for the magnetic cycling along the long side of Hall bar, while a tilted elliptic M–H loop is detected along the short side. This demonstrates that the ultrathin YIG(3 nm)/Pt sample has strongly magnetic anisotropy with respect to in-plane easy magnetic axis. The anisotropy results from growth-specific factors,[31] such as lattice strain,[32] small misorientation of the film surface normal with respect to the [111] direction, slightly off-normal plasma plume orientation, or uniaxial in-plane strain due to growth temperature gradients.[33] The uniaxial in-plane anisotropy of ultrathin YIG film caused by local strain change during pulsed laser deposition depends strongly on the thickness of YIG layer. Therefore, compared with YIG(5 nm)/Pt sample, the YIG(3 nm)/Pt sample has strong magnetic anisotropy.

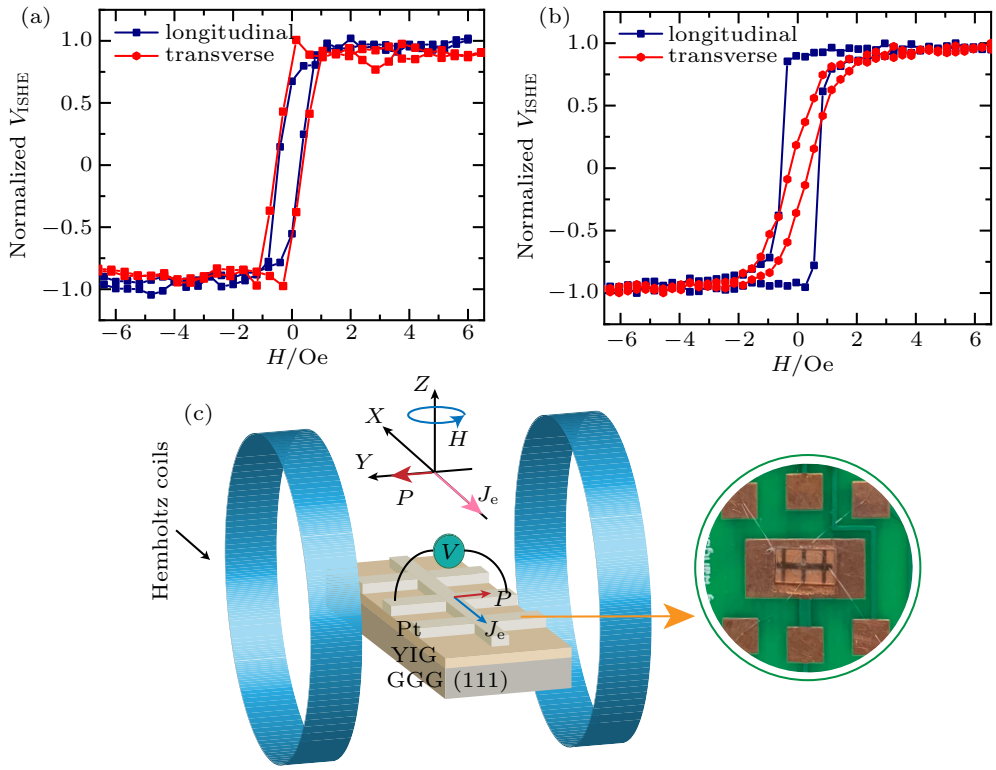

Fig. 1. [(a) and (b)] Normalized $V_{\rm ISHE}$–H curves of YIG(5 nm)/Pt and YIG(3 nm)/Pt bilayers, respectively. (c) Schematic diagram of experimental setup with inset indicating optical image of YIG(3 nm)/Pt sample. The unit 1 Oe = 79.5775 A·m^{-1}.

During the measurement, a rotating external magnetic field $\boldsymbol{H}$ was applied to the in-plane direction of film. The sample was placed in aluminum electromagnetic shielding to improve the signal-to-noise ratio during the measurement. A schematic of the experiment setup is shown in Fig. 1(c). The inset of Fig. 1(c) shows the optical image of YIG(3 nm)/Pt sample. Driving current (J_e) was applied along the x-axis Pt. Two electrodes were aligned along the y axis to detect the voltage and measure the SMR effect. This setup has been used because the transversal resistivity V_y presented a low background signal and thus gave a high signal-to-noise ratio.[23,34] The angle between the external magnetic field and J_e is defined as β, and we define β' as the angle between the magnetic moment ($\boldsymbol{M}$) and J_e. The value of SMR is sensitively dependent on

the direction between $\boldsymbol{M}$ and J_e. The transversal magnetoresistance is given by[24]

$$\rho_{xy} = \Delta\rho \sin(2\beta'), \tag{1}$$

where $\Delta\rho$ is the magnitude of resistivity change as a function of magnetization orientation. Therefore, the magnetic moment direction can be obtained from the angle β' by using Eq. (1).

3. Results and discussion

Because the value of SMR changes periodically (180°), we only examine the SMR curves in one period ($\beta = 0°$–180°). When a large external magnetic field of 1500 Oe is applied to the YIG(5 nm)/Pt sample, the magnetization lies exactly along the direction of external field, *i.e.*, $\beta' = \beta$. As shown in Fig. 2(a), the experimental value of SMR can be well fitted by Eq. (1). Even when J_e is increased to 1×10^6 A/cm^2, the shape of SMR curve does not change and still remains highly consistent with the theoretical curve. This indicates that when the external magnetic field is large enough, the applied torque of external magnetic field on $\boldsymbol{M}$ is larger than the torque due to the driving current J_e. The orientation of magnetic moment is mainly determined by the external magnetic field $\boldsymbol{H}$. The influence of SOT on the $\boldsymbol{M}$ is negligible. Similarly, the SMR curves are in consistence with Eq. (1) in the YIG(20 nm)/Pt sample (see Fig. S1). When the film of YIG grows, the direction of $\boldsymbol{M}$ cannot be changed because the SOT is not strong enough to reorient $\boldsymbol{M}$.

Figure 2(b) shows the dependence of SMR on magnetic field angle (β) when the injected current is 1×10^6 A/cm^2. It is quite obvious that when the field decreases to 6 Oe and 4 Oe, the SMR curves clearly no longer follow Eq. (1), deviating from the theoretical predicted values. Therefore, when the field decreases to a few Oe, the effect of injected current J_e on the magnetic moment of YIG cannot be neglected. The magnetization of YIG is not saturated with H decreasing constantly, and irregular SMR curves are observed to cover up the current effect (see Fig. S2). So, we will discuss only the SMR curves when the external field is above the saturation field.

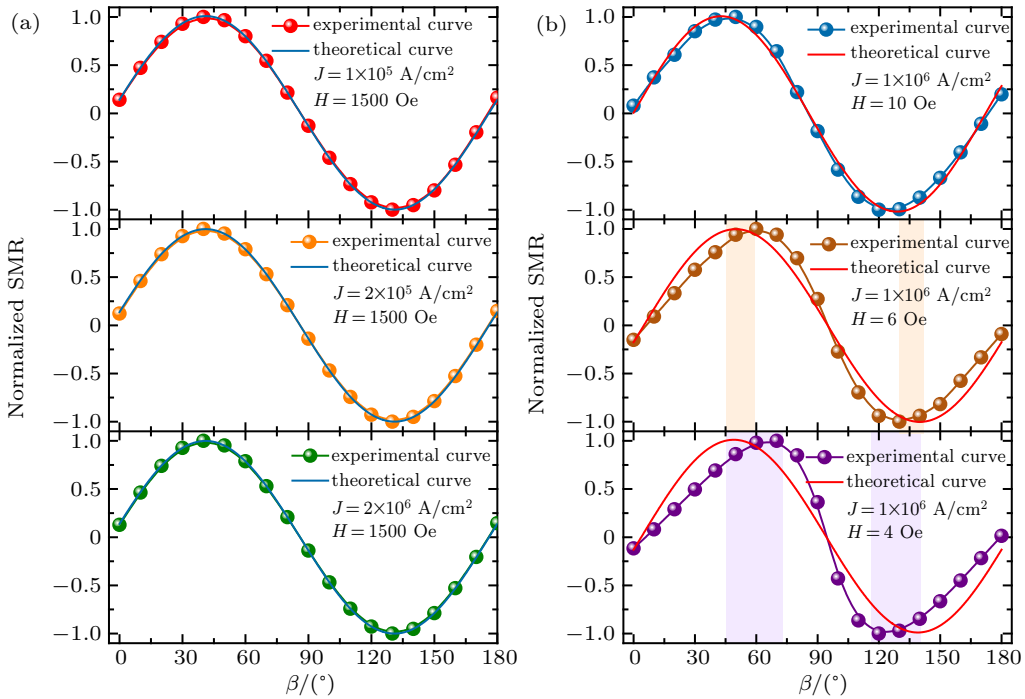

Fig. 2. (a) YIG(5 nm)/Pt SMR curves with different values of J_e under external magnetic field of $H = 1500$ Oe. (b) YIG(5 nm)/Pt SMR curves with $J_e = 1\times10^6$ A/cm^2 *versus* in-plane rotation angle under magnetic field of 10, 6, and 4 Oe.

The SMRs under different values of J_e in the YIG(5 nm)/Pt sample are also measured when the external magnetic field is fixed at 4 Oe. The result is still in agreement with the theoretical value when the driving current $J_e = 1\times10^5$ A/cm^2 (see Fig. 3(a)). However, when J_e increases to 2×10^5 A/cm^2, the experimental data have a significant shift toward higher angles relative to the theoretical values (see Fig. 3(b)). If the current further increases to 1×10^6 A/cm^2 and 2×10^6 A/cm^2 separately, the degree of deviation slightly increases as shown in Figs. 3(c) and 3(d). This indicates that the $\boldsymbol{M}$ no longer exactly follows the external magnetic field direction if J_e is large enough although the 4-Oe field is above the saturation field of sample. Based on Eq. (1), the actual angle (β') between the $\boldsymbol{M}$ and J_e can be calculated. Figures 4(a) and 4(b) show the relationship between the theoretical value β and the actual value β'. As shown in Fig. 4(a), when J_e is 1×10^5 A/cm^2, β' is synchronized with β. The magnitude of change in β' is essentially the same as the angle variation

of external magnetic field. The torque for modulating the direction of magnetic moment is provided mainly by the external magnetic field. When the driving current J_e increases to 2×10^5, 1×10^6, and 2×10^6 A/cm^2 separately, β and β' deviate from each other. The variations in β' lag behind β when β is 0°–90°, *i.e.*, $\beta > \beta'$, while β' gets ahead of β in a range of 90°–180°, *i.e.*, $\beta < \beta'$. This implies that the direction of $\boldsymbol{M}$ does not completely coincide with the external magnetic field. Hence, under a low magnetic field, the torque applied to the magnetic moment by the external magnetic field is not the only significant torque for determining the direction of $\boldsymbol{M}$ alignment.

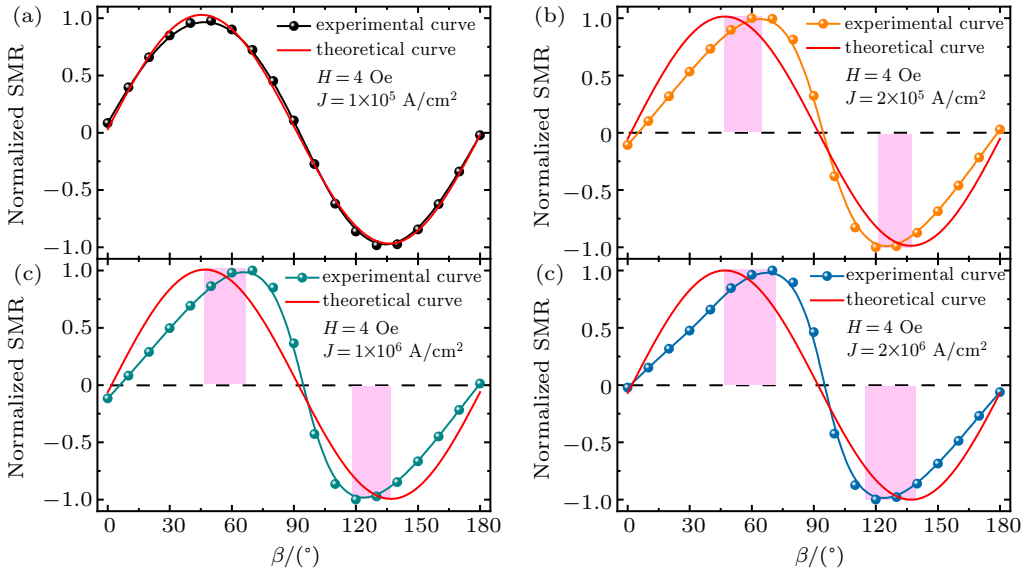

Fig. 3. Curves of normalized SMR–β *versus* β for the YIG(5 nm)/Pt sample with driving current $J_e = 1\times10^5$ (a), 2×10^5 (b), 1×10^6 (c), and 2×10^6 A/cm^2 (d) under external magnetic field 4 Oe.

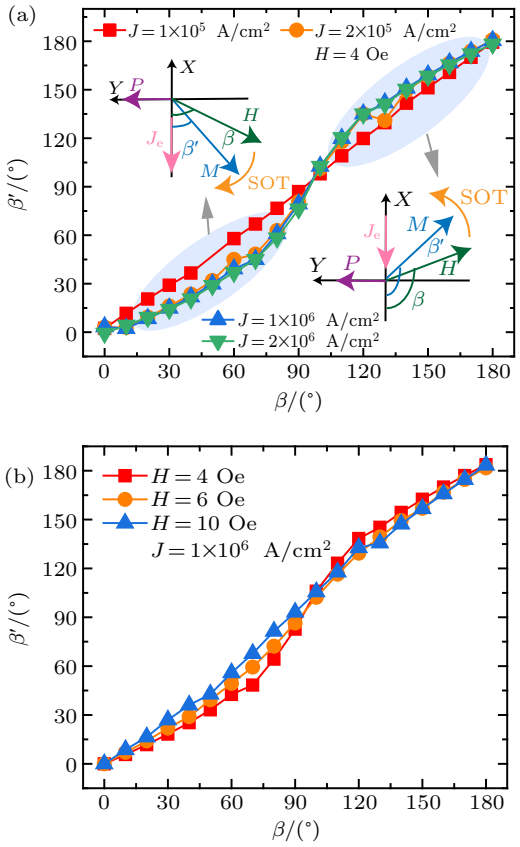

Fig. 4. Relationships between theoretical value β and actual value β' in YIG(5 nm)/Pt sample under different values of (a) driving current J_e and (b) $\boldsymbol{H}$, with insert showing that antidamping torque is applied to $\boldsymbol{M}$, causing $\boldsymbol{M}$ to deviate from the direction of external magnetic field $\boldsymbol{H}$.

The similar phenomenon is also observed in Fig. 4(b). The current amplitude for writing is fixed at 1×10^6 A/cm^2. For $H = 10$ Oe, β' is nearly equal to β, the magnetization rotates coherently with magnetic field. On the other hand, if the external magnetic field further reduces 6 Oe and 4 Oe, β' gradually deviates from β. It means that the torque produced by injected current J_e has an influence on $\boldsymbol{M}$.

Therefore, a large current in Pt will cause the magnetization in YIG to be reorientated, and the reason needs to be explored in depth. As is well known, an Oersted field and Joule heating effect will emerge when a large current density will be applied. However, because the direction of J_e remains unchanged in this experiment, the direction of the Oersted field which is determined by J_e is also constant. If the Oersted field leads the magnetization to be reorientated, the change period of SMR should be 360° rather than 180° which is not the case in our measurement results. Meanwhile, the Joule heat produced by J_e is the same. If the deviation of the SMR curve is caused by Joule heat, the SMR curves of YIG(20 nm)/Pt should be the same as that of YIG(5 nm)/Pt which is not consistent with the experimental phenomenon (see Fig. 2 and Fig. S1). Therefore, the reorientation of the magnetization does not origin from the Oersted field nor Joule heating effect.

A further insight into this reorientation process can be gained analyzing in depth the SOT in the SMR curves. Since the directions of field-like torques are out-of-plane, it is worth

noting that reactive field-like torques are forbidden due to the in-plane magnetization.[10] of YIG. The inset of Fig. 4(a) shows the change of actual angle β' under the external magnetic field $\boldsymbol{H}$ and the antidamping torques when the β is below and above 90°, respectively. The $\boldsymbol{M}$ is aligned along the direction of external magnetic field $\boldsymbol{H}$ when the external magnetic field is sufficient to saturate the YIG magnetization as shown in Fig. 2(a). However, under a low external magnetic field and the application of a large J_e to Pt, the spin accumulation near the YIG/Pt interface due to the spin Hall effect will generate antidamping torques τ_{DL} perpendicular to the $\boldsymbol{M}$. The τ_{DL} causes the $\boldsymbol{M}$ to deviate from the direction of the external magnetic field. The detailed relationship between β and β' is presented in the inset of Fig. 4(a). When $\beta = 0°$–$90°$, the τ_{DL} induces clockwise force, and so β' is less than β and the actual value $\rho_{xy} = -\Delta\rho\sin(2\beta')$ lags behind the theoretical value $\rho_{xy} = -\Delta\rho\sin(2\beta)$. When $\beta = 90°$, *i.e.*, $\boldsymbol{M}$ is parallel to spin polarization, antidamping torque on $\boldsymbol{M}$ becomes zero, leading the $\boldsymbol{M}$ to be aligned with the direction of the external magnetic field, *i.e.*, $\beta' = \beta$. For $\beta > 90°$, the antidamping torque is anticlockwise, resulting in $\beta' > \beta$. By calculating the corresponding ρ_{xy}, it can be found that the actual value of SMR is ahead of the theoretical value. It is thus inferred that the antidamping torque always aligns $\boldsymbol{M}$ with the direction parallel to J_e.

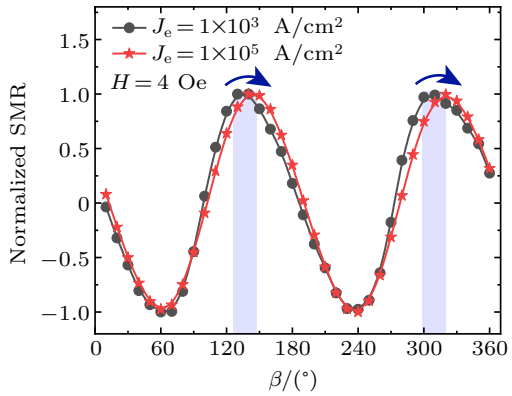

Fig. 5. Curves of normalized SMR *versus* β for driving current $J_e = 1\times10^3$ A/cm^2 (grey dots) and 1×10^5 A/cm^2 (red dots) along easy axis of YIG(3 nm)/Pt sample under external magnetic field $\boldsymbol{H} = 4$ Oe.

In order to further explore the effect of antidamping torque on the alignment of $\boldsymbol{M}$, we also conduct the measurement on the YIG(3 nm)/Pt sample (see Fig. 5). As shown in Fig. 1(b), the ultrathin YIG possesses strong easy-plane anisotropy, which is consistent with a recent report by Mendil *et al.*[31] They found that the magnetic properties and domain configurations of epitaxial YIG (111) films depend strongly on the thickness of YIG layer, and a strong easy-plane anisotropy field was measured in the ultrathin YIG. This anisotropy is also reflected in our ultrathin YIG(3 nm)/Pt by the reorientation of SMR (grey dots in Fig. 5) measured at a current of 1×10^3 A/cm^2. As J_e increases to 1×10^5 A/cm^2, the red dots representing SMR deviate from the grey dots and shift towards higher angles. The offset direction is consistent with that in YIG (5 nm)/Pt. Therefore, the antidamping torques still exist in the magnetic anisotropy in YIG(3 nm)/Pt.

We also notice that in the work by Mendil *et al.*[26] a sudden 180° reversal of the magnetization from the positive to the negative direction of easy axis is present when applied magnetic field is 60 μT. Furthermore, they also observed that as the magnitude of the external magnetic field B_{ext} and current-induced B_I are in the range of tens of μT, the Oersted field B_I shifts to the magnetization reversal and changes the period of transversal spin Hall magnetoresistance R_{xy} versus field direction curves from 180° to 360°. In this work, however, since the applied magnetic field is as high as 4 Oe which is much larger than tens of μT, the direction of magnetization is not reversed, but deviate from the external field direction. According to our analysis, under higher field, SOT plays a more important role than the Oersted field in the reorientation of magnetization.

4. Conclusion and perspectives

In this work, we provide an experimental evidence for magnetization reorientation induced by SOT in a YIG/Pt system. The SMR measurements under different external magnetic fields and different values of driving current J_e accurately characterize the $\boldsymbol{M}$ direction change caused by antidamping torques. Our investigation indicates that the variations of the YIG magnetic properties may be strongly influenced by the driving current J_e, even when the external magnetic field is above the saturation field of sample. It is concluded that the SOT is an effective method to achieve in-plane magnetic moment reorientation and may be used in the future study to improve the performances of YIG-based spintronic devices.

Acknowledgment

We would like to thank the Analytical & Testing Center of Northwestern Polytechnical University for PPMS characterization.

References

[1] Slonczewski J C 1996 *J. Magn. Magn. Mater.* **159** L1
[2] Berger L 1996 *Phys. Rev. B* **54** 9353
[3] Katine J A, Albert F J, Buhrman R A, Myers E B and Ralph D C 2000 *Phys. Rev. Lett.* **84** 3149
[4] Kiselev S I, Sankey J C, Krivorotov I N, Emley N C, Schoelkopf R J, Buhrman R A and Ralph D C 2003 *Nature* **425** 380
[5] Liu L, Pai C F, Li Y, Tseng H W, Ralph D C and Buhrman R A 2012 *Science* **336** 555
[6] Ralph D C and Stiles M D 2008 *J. Magn. Magn. Mater.* **320** 1190
[7] Feng X Y, Zhang Q H, Zhang H W, Zhang Y, Zhong R, Lu B W, Cao J W and Fan X L 2019 *Chin. Phys. B* **28** 107105
[8] Li S, Goolaup S, Kwon J, Luo F, Gan W and Lew W S 2017 *Sci. Rep.* **7** 972
[9] Ma Q, Li Y, Gopman D B, Kabanov Y P, Shull R D and Chien C L 2018 *Phys. Rev. Lett.* **120** 117703

[10] Chen X Z, Zarzuela R, Zhang J, Song C, Zhou X F, Shi G Y, Li F, Zhou H A, Jiang W J, Pan F and Tserkovnyak Y 2018 *Phys. Rev. Lett.* **120** 207204
[11] Stiles M D and Zangwill A 2002 *Phys. Rev. B* **66** 81
[12] Liu L, Lee O J, Gudmundsen T J, Ralph D C and Buhrman R A 2012 *Phys. Rev. Lett.* **109** 096602
[13] Amin V P and Stiles M D 2016 *Phys. Rev. B* **94** 104419
[14] Manchon A and Zhang S 2009 *Phys. Rev. B* **79** 094422
[15] Zhao X, Zhang X, Yang H, Cai W, Zhao Y, Wang Z and Zhao W 2019 *Nanotechnology* **30** 335707
[16] Sheng Y, Zhang N, Wang K Y and Ma X Q 2018 *Acta Phys. Sin.* **67** 117501 (in Chinese)
[17] Fan Y, Upadhyaya P, Kou X, Lang M, Takei S, Wang Z, Tang J, He L, Chang L-T, Montazeri M, Yu G, Jiang W, Nie T, Schwartz R N, Tserkovnyak Y and Wang K L 2014 *Nat. Mater.* **13** 699
[18] Chen X, Zhou X, Cheng R, Song C, Zhang J, Wu Y, Ba Y, Li H, Sun Y, You Y, Zhao Y and Pan F 2019 *Nat. Mater.* **18** 931
[19] An K, Olsson K S, Weathers A, Sullivan S, Chen X, Li X, Marshall L G, Ma X, Klimovich N, Zhou J, Shi L and Li X 2016 *Phys. Rev. Lett.* **117** 107202
[20] Wang S H, Li G, Guo E J, Zhao Y, Wang J Y, Zou L K, Yan H, Cai J W, Zhang Z T, Wang M, Tian Y Y, Zheng X L, Sun J R and Jin K X 2018 *Phys. Rev. Mater.* **2** 051401
[21] Serga A A, Chumak A V and Hillebrands B 2010 *J. Phys. D: Appl. Phys.* **43** 264002
[22] Uchida K, Takahashi S, Harii K, Ieda J, Koshibae W, Ando K, Maekawa S and Saitoh E 2008 *Nature* **455** 778
[23] Chen Y-T, Takahashi S, Nakayama H, Althammer M, Goennenwein S, Saitoh E and Bauer G 2013 *Phys. Rev. B* **87** 144411
[24] Nakayama H, Althammer M, Chen Y T, Uchida K, Kajiwara Y, Kikuchi D, Ohtani T, Geprags S, Opel M, Takahashi S, Gross R, Bauer G E, Goennenwein S T and Saitoh E 2013 *Phys. Rev. Lett.* **110** 206601
[25] Liu Q, Meng K, Cai Y, Qian X, Wu Y, Zheng S and Jiang Y 2018 *Appl. Phys. Lett.* **112** 022402
[26] Mendil J, Trassin M, Bu Q, Fiebig M and Gambardella P 2019 *Appl. Phys. Lett.* **114** 172404
[27] Lotze J, Huebl H, Gross R and Goennenwein S T B 2014 *Phys. Rev. B* **90** 174419
[28] Uchida K, Adachi H, Ota T, Nakayama H, Maekawa S and Saitoh E 2010 *Appl. Phys. Lett.* **97** 172505
[29] Uchida K, Ishida M, Kikkawa T, Kirihara A, Murakami T and Saitoh E 2014 *J. Phys.: Condens. Matter* **26** 343202
[30] Magginetti D, Tian K and Tiwari A 2017 *Solid State Commun.* **249** 34
[31] Mendil J, Trassin M, Bu Q, Schaab J, Baumgartner M, Murer C, Dao P T, Vijayakumar J, Bracher D and Bouillet C 2019 *Phys. Rev. Mater.* **3** 034403
[32] Wang C T, Liang X F, Zhang Y, Liang X, Zhu Y P, Qin J, Gao Y, Peng B, Sun N X and Bi L 2017 *Phys. Rev. B* **96** 224403
[33] Krichevtsov B B, Gastev S V, Suturin S M, Fedorov V V, Korovin A M, Bursian V E, Banshchikov A G, Volkov M P, Tabuchi M and Sokolov N S 2017 *Sci. Technol. Adv. Mat.* **18** 351
[34] Wang S, Li G, Wang J, Tian Y, Zhang H, Zou L, Sun J and Jin K 2018 *Chin. Phys. B* **27** 117201